Dalton Transactions

Accepted Manuscript

ROYAL SOCIETY OF CHEMISTRY

www.rsc.org/dalton

Mn(II) complexes of different nuclearity: synthesis, characterization and catecholase-like activity

Prateeti Chakraborty,*[a, e] Ishani Majumder,[a] Kazi Sabnam Banu,[a] Bipinbihari Ghosh,[b] Hulya Kara,[c] Ennio Zangrando,*[d] and Debasis Das*[a]

[a]*Department of Chemistry, University of Calcutta, 92, A. P. C. Road, Kolkata – 700009, India*

[b]*Department of Chemistry, Indian Institute of Engineering, Science and Technology, Shibpur, Howrah-711103, India*

[c]*Department of Physics, Faculty of Science and Art, Balikesir University, 10145 Balikesir, Turkey*

[d] *Department of Chemical and Pharmaceutical Sciences, University of Trieste, Via L. Giorgieri 1, 34127 Trieste, Italy*

[e] *Department of Chemistry, Amity University, Newtown, Kolkata, West Bengal 700156, India*

ABSTRACT

Two "end-off" compartmental ligands, 2-formyl-4-chloro-6-N-ethylmorpholine-iminomethyl-phenol (HL1) and 2-formyl-4-methyl-6-N-ethylpyrrolidine-iminomethyl-phenol (HL2) have been designed and three complexes of Mn(II), one Mono-, one di- and other polynuclear, namely $Mn(L1)(SCN)_2(H_2O)]$ (**1**), $[Mn_2(L1)(OAc)_2](BPh_4)]$ (**2**), and $[Mn_2(L2)(OAc)_2(dca)]_n$(**3**) have been synthesized and structurally characterized. Variable temperature magnetic study of **2** and **3** have been performed and data analyses reveal that Mn centers are antiferromagetic coupled with J = - 9.15 cm^{-1} and J = - 46.89, respectively. Catecholase activity of all the complexes have been investigated using 3,5-di-*tert*-butyl catechol (3,5-DTBC). All are highly active with activity order on the basis of k_{cat} value is **2**>**1**>**3**. In order to unveil whether metal centered redox participation or radical pathway is responsible for the catecholase-like activity of the complexes detailed EPR and cyclic voltametric (CV) study have been performed. In addition to six line EPR spectrum characteristic to Mn(II) an additional peak at g~2 is observed when the EPR study is done with the mixture of 3,5-DTBC and catalyst, suggesting the formation of organic radical

most likely ligand centered. CV experiment with the mixture of 3,5-DTBC and catalyst reveals ligand centered reduction rather than reduction of Mn(II) to Mn(I). It is thus inferred that complexes **1-3** show catecholase-like activity due to radical generation.

Introduction

The oxidation of organic substrates by metalloenzymes, that activate molecular oxygen under mild conditions, has received vast deal of concentration in the arena of industrial and synthetic processes.[1-4] As a result many groups tried to build up the finest model of transition metal complexes able to mimic oxidase activity of metalloenzymes. One of the foremost enzymes that play a key role in these oxidation reactions is catechol oxidase (CO), a lesser well known member of the type-III copper proteins originate in plant tissues and crustaceans. This process, known as catecholase activity, allows to catalyze the oxidation of a wide range of o-diphenols (catechols) to the corresponding o-quinones (Scheme 1).[5-8] Recently our group has got admirable results while mimicking catecholase activity with phenol based compartmental ligand complexes of Ni(II),[9] Cu(II)[10,11] and Zn(II)[12]. In this manuscript we widen our work by using manganese, one of the most important trace transition element in biological system being present in numerous metalloenzymes of varied nuclearity. From literature survey, it is possible to recognize that some complexes of Mn(III)[13], Mn(IV)[14], and a very few ones of Mn(II)[15] are found to mimic catecholase-like activity, and these derivatives were generally made up from salen-type Schiff bases, tripodal ,and pyridine-containing ligands etc, while phenol based compartmental ligands have been very rarely used. Our earlier studies with Mn(III) discloses metal-centered redox participation as a most probable pathway for the catecholase activity of the model compounds.[13b] In case of Mn(II) complexes[15] although we found excellent catalytic activities but failed to evaluate the plausible catalytic mechanism. That failure inspires us to synthesize new Mn(II) complexes to explore that untouched arena of catecholase activity study and thereby to unveil the most probable mechanistic pathway. In order to reach to our goal the ligands of our choice in the present study are two phenol based compartmental ligands, namely 2-formyl-4-chloro-6-N-ethylmorpholine-iminomethyl-phenol (HL1) and 2-formyl-4-methyl-6-N-ethylpyrrolidine-iminomethyl-phenol (HL2). We have prepared three Mn(II) complexes having different

nuclearities, i.e. $[Mn(L1)(SCN)_2(H_2O)]$ (**1**), $[Mn_2(L1)(OAc)_2](BPh_4)]$ (**2**), and $[Mn_2(L2)(OAc)_2(dca)]_n$ (**3**), structurally characterized them and have studied their catecholase-like activity in DMSO solvent with 3,5-di-*tert*-butylcatechol (3,5-DTBC) as substrate. EPR and cyclic voltametric study help us to understand the origin of the catecholase-like activity of our Mn(II) complexes. Variable temperature magnetic study on complexes **2** and **3** has also been performed since the compounds of phenol based compartmental ligands are well known for their stimulating magnetic properties.[16-19] This examination of magnetic properties of such compounds helps not only in further understanding the relations between magnetic coupling centers in metalloproteins and enzymes, but also to extend the knowledge of molecular magnetism.

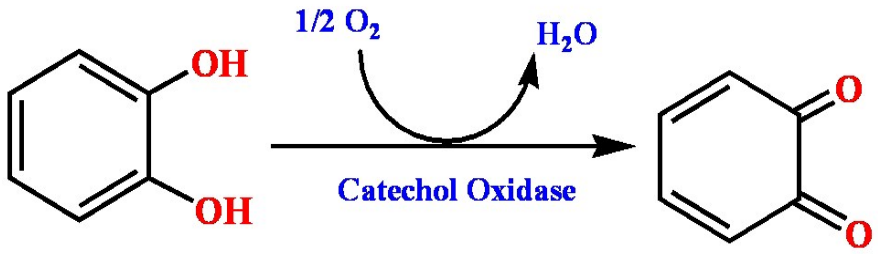

Scheme. 1 Reaction Pathway of the Oxidation Catalyzed by CO.

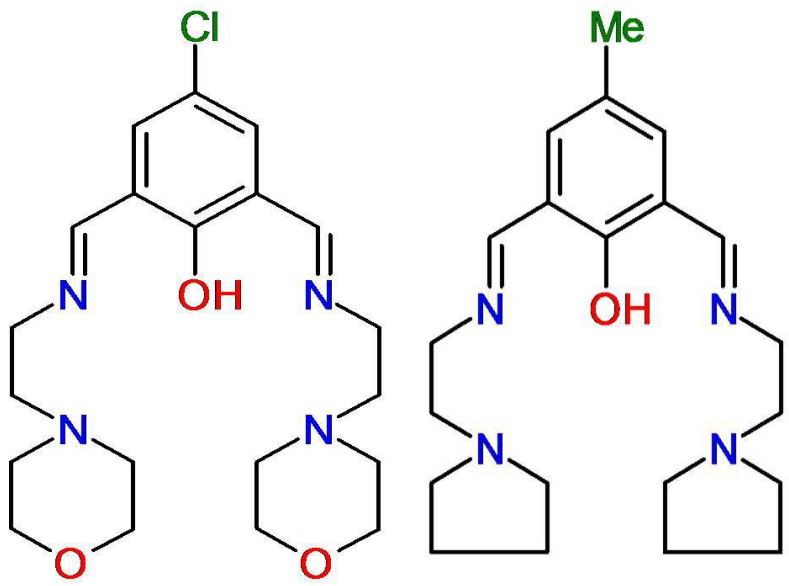

HL1 **HL2**

Fig. 1 Structure of the two Synthesized Compartmental Ligands.

Results and Discussion

Synthesis, Rationalization, and Characterization of the Metal-Complexes.

Three manganese (II) complexes (**1-3**) were prepared by adopting the template synthesis technique by treating a methanolic solution of corresponding manganese salts with the Schiff base formed in situ between 2,6-diformyl-4-R-phenol (where R= chloro, methyl) and the diamines and structurally characterized by single crystal X-ray diffraction (*vide infra*). FT-IR spectral study reveals that all complexes exhibit bands due to the C=N stretch in the range 1630−1648 cm^{-1} and skeletal vibration in the range 1545−1555 cm^{-1}. The presence of coordinated SCN^- anion in complex **1** has been assigned by a broad band in the region of 2065 cm^{-1}. In complex **2** the OAc^- anions show bands at 1483 cm^{-1} and in complex **3** OAc^- anions and dicyanamide show bands at 1488 and 2165 cm^{-1}, respectively. Electronic spectra of all complexes studied in DMSO medium display very similar absorption bands in the range 375-425 nm. The observed strong higher energy single band (between 375 and 425 nm) is due to combination of both phenoxido−Mn(II) and hydroxido−Mn(II) LMCT bands. Room temperature

(300 K) magnetic moment calculation reveals that (5.96 μB for complex **1**, 8.37 μ_B and 8.19 μ_B for complex **2** and **3** respectively) Mn(II) in all complexes is in high spin state.

Crystal Structure Descriptions

The crystal structure analysis showed the formation of a mononuclear neutral species, $[Mn(HL1)(SCN)_2(H_2O)]$, due to the protonation of one of the imine nitrogen atoms. An ORTEP drawing is depicted in Figure 1, and a selection of coordination bond distances and angles is reported in Table 1. The metal is chelated by ligand HL1 through the phenoxo oxygen atom, the imine-nitrogen and amine donor of the morpholine ring with Mn-O and Mn-N bond distances of 2.1222(14), 2.2075(18), and 2.387(13)Å, respectively. The latter value refers to the coordinated morpholine moiety at higher occupancy (see experimental section).The distorted octahedral coordination sphere is completed by an aqua ligand and two isothiocyanate anions (Mn-O1w = 2.3692(18), Mn-NCS = 2.163(2) and 2.154(2) Å. The distortions in the coordination bond angles are attributable to a strength in the HL1 chelation and the value of O1-Mn-N3 (of 156.5(2)°) is the more deviating from ideal geometry (Table. 1). The protonated imino nitrogen N1 forms an intramolecular H-bond with the phenolato oxygen O1 (N...O distance 2.598(2) Å), and the water molecule is engaged in weak H-bonding with N4 and S2 of a symmetry related complex at x,1/2−y, −1/2+z (O1w…N4 = 3.130(3) and O1w…S2 = 3.330(2)Å) to form a polymeric species developed parallel axis *a*. The structural data of complex **1** are comparable to those detected in the corresponding species having a pyridine replacing the morpholine ring reported by us a few years ago.[15]

Table 1. Coordination bond lengths (Å) and angles (°) for complex **1**.

Mn-O(1)	2.1222(14)	Mn-N(3) *	2.387(13)
Mn-O(1w)	2.3692(18)	Mn-N(3b) *	2.413(13)
Mn-N(1)	2.2075(18)	Mn-N(5)	2.163(2)
		Mn-N(6)	2.154(2)

O(1)-Mn-N(6)	89.73(7)	N(5)-Mn-O(1w)	176.52(8)
O(1)-Mn-N(5)	89.35(8)	N(1)-Mn-O(1w)	82.69(7)
N(6)-Mn-N(5)	93.29(9)	O(1)-Mn-N(3)	156.5(2)
O(1)-Mn-N(1)	82.07(6)	N(6)-Mn-N(3)	111.3(2)
N(6)-Mn-N(1)	163.57(8)	N(5)-Mn-N(3)	85.2(2)
N(5)-Mn-N(1)	100.79(9)	N(1)-Mn-N(3)	76.6(2)

O(1)-Mn-O(1w)	91.18(7)	O(1w)-Mn-N(3)	95.7(2)
N(6)-Mn-O(1w)	83.28(8)		

* N3 and N3b represent the donor of the disordered coordinated morpholine. Only bond angles involving the higher occupancy is reported.

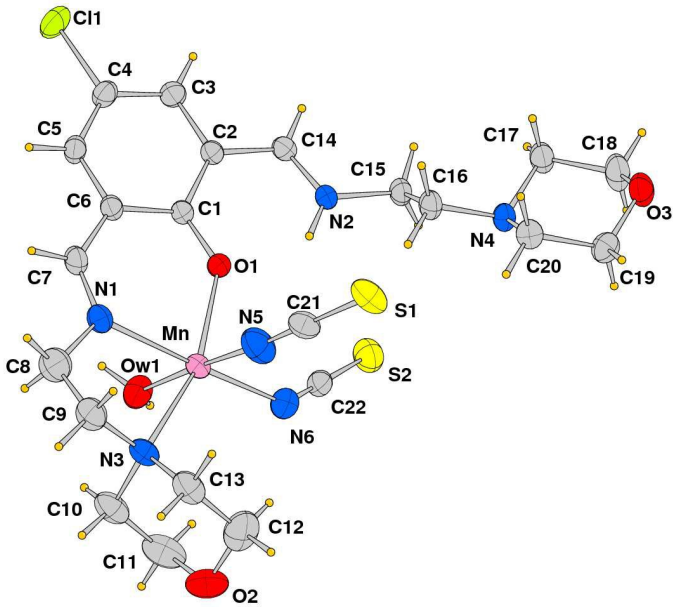

Fig. 2 ORTEP drawing (ellipsoid probability at 30%) with atom labels of complex **1**. (Of the disordered coordinated morpholine only that at higher occupancy is shown).

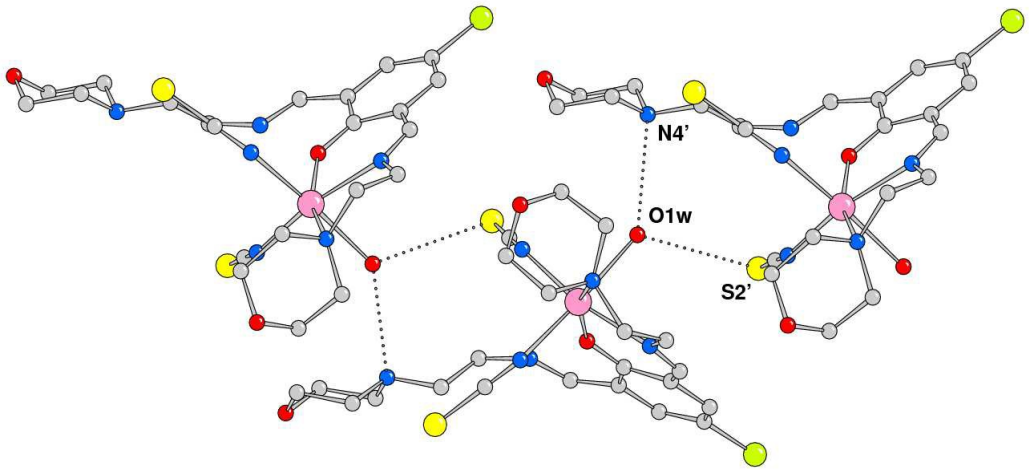

Fig. 3 Complexes **1** connected through H-bonds by the coordinated water molecule (primed atoms at x,1/2−y, −1/2+z).

The structural analysis revealed that compound **2** is a dinuclear cationic species and the unit cell contains two independent complexes located on a crystallographic mirror plane, normal to the phenolato ring plane passing in between the manganese atoms, beside a BPh_4 anion. An ORTEP view of one of the two the μ-phenoxo-di-μ-acetato-dimanganese(II) complex with atom labeling scheme of independent atoms is shown in Fig. 4. In both species the metal ions exhibit a distorted trigonal bipyramidal coordination sphere comprising in the equatorial plane the imine nitrogen donor N1 and acetate oxygens O2 and O3, while the phenoxido-bridged oxygen O1, and morpholine amine nitrogen N2 occupy the axial positions (N4, O5, O6 and O4, N5 are the corresponding atoms in the second complex). The Mn-O and Mn-N bond distances reported in Table 2 indicate comparable values for the two independent complexes with the exception of the Mn-N(amino) bond that differs by ca. 0.1 Å (2.442(3) vs 2.335(3)Å). It is worth of note the shorter Mn-O(acetate) bond lengths (mean value 2.176 Å with respect the Mn-O(oxo) ones that average to 2.039 Å. Correspondingly a difference is observed in the intermetallic distance being of 3.3455(9) and 3.2194(8)Å, respectively in the two complexes.

Table 2. Coordination bond lengths (Å) and angles (°) for complex **2**.

Mn(1)-O(1)	2.197(2)	Mn(2)-O(5)	2.156(2)
Mn(1)-O(2)	2.030(3)	Mn(2)-O(6)	2.058(3)
Mn(1)-O(3)	2.020(3)	Mn(2)-O(7)	2.048(3)
Mn(1)-N(1)	2.117(3)	Mn(2)-N(4)	2.092(3)
Mn(1)-N(2)	2.442(3)	Mn(2)-N(5)	2.335(3)
Mn(1)-Mn(1)'	3.3455(9)	Mn(2)-Mn(2)'	3.2194(8)
O(3)-Mn(1)-O(2)	115.71(15)	O(7)-Mn(2)-O(6)	130.85(18)
O(3)-Mn(1)-N(1)	123.69(15)	O(7)-Mn(2)-N(4)	115.63(13)
O(2)-Mn(1)-N(1)	120.46(11)	O(6)-Mn(2)-N(4)	113.52(18)
O(3)-Mn(1)-O(1)	95.80(13)	O(7)-Mn(2)-O(5)	92.16(12)
O(2)-Mn(1)-O(1)	93.10(11)	O(6)-Mn(2)-O(5)	92.44(14)
N(1)-Mn(1)-O(1)	85.12(9)	N(4)-Mn(2)-O(5)	84.96(11)
O(3)-Mn(1)-N(2)	89.64(11)	O(7)-Mn(2)-N(5)	91.86(11)
O(2)-Mn(1)-N(2)	99.89(10)	O(6)-Mn(2)-N(5)	95.69(13)
N(1)-Mn(1)-N(2)	77.70(10)	N(4)-Mn(2)-N(5)	80.44(11)
O(1)-Mn(1)-N(2)	162.09(9)	O(5)-Mn(2)-N(5)	165.19(10)

Primed atoms at x, 1/2−y, z.

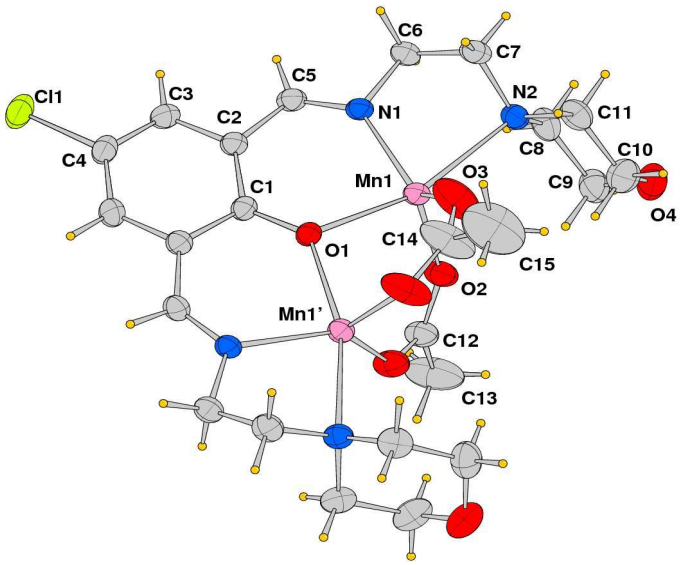

Fig. 4 ORTEP drawing (ellipsoid probability at 30%) with atom labels of one of the two independent cationic complexes of compound **2**. The complex is located on a crystallographic symmetry plane.

By using the coordinating dicyanoamide as counteranion, the metals assume a distorted octahedral geometry in dinuclear complex **3**. Each metal is chelated by Schiff base ligand HL2 through the phenoxo oxygen atom, the imine-nitrogen and amine donor of the pyrrolidine ring. In addition the coordination sphere is filled by two oxygens from different acetate anions and a nitrogen donor from a bridging dca ligand. With respect to complex **2**, the Mn-O and Mn-N bond distances are here slightly longer. In particular the Mn-N(imine) bond distances are of 2.189(9) and 2.192(8)Å which must be compared a mean value of 2.104 Å in **2**. Here the acetate anions bridge the metals in asymmetric fashion, with a long bond length with Mn1 (2.184(8)Å) and a shorter one with Mn2 (2.091(7)Å),and vice versa for the other anion (2.066(8)and 2.157(9)Å, respectively). The Mn-O(oxo) and Mn-N(amine) bond lengths are comparable to those measured in **2**. As mentioned above the dca anions bridge metals of different complexes giving rise to a coordination polymer running parallel to axis *a*. The dca CN groups coordinate the metals with different CN-Mn angles, of 148.4(12) and 166.3(11)°, where the latter shows an almost linear

coordination. The intermetallic Mn1-Mn2 in this neutral complex, of 3.389(3) Å, is slightly longer than the value measured in **2**.

Table 3. Coordination bond lengths (Å) and angles (°) for complex **3**

Mn(1)-O(1)	2.151(8)	Mn(2)-O(1)	2.162(7)
Mn(1)-O(2)	2.184(8)	Mn(2)-O(3)	2.091(7)
Mn(1)-O(4)	2.066(8)	Mn(2)-O(5)	2.157(9)
Mn(1)-N(1)	2.189(9)	Mn(2)-N(2)	2.192(8)
Mn(1)-N(3)	2.395(9)	Mn(2)-N(4)	2.421(9)
Mn(1)-N(5)	2.256(11)	Mn(2)-N(7)'	2.231(11)
Mn(1)-Mn(2)	3.389(3)		
O(4)-Mn(1)-O(1)	106.6(3)	O(3)-Mn(2)-O(1)	103.3(3)
O(4)-Mn(1)-O(2)	88.7(3)	O(3)-Mn(2)-O(5)	90.8(3)
O(1)-Mn(1)-O(2)	93.1(3)	O(5)-Mn(2)-O(1)	92.4(3)
O(4)-Mn(1)-N(1)	170.6(3)	O(3)-Mn(2)-N(2)	172.5(3)
O(1)-Mn(1)-N(1)	82.6(3)	O(5)-Mn(2)-N(2)	93.9(3)
O(2)-Mn(1)-N(1)	92.8(3)	O(1)-Mn(2)-N(2)	82.4(3)
O(4)-Mn(1)-N(5)	87.8(4)	O(3)-Mn(2)-N(7)'	88.7(4)
O(2)-Mn(1)-N(5)	176.5(4)	O(5)-Mn(2)-N(7)'	177.0(4)
O(1)-Mn(1)-N(5)	88.1(3)	O(1)-Mn(2)-N(7)'	90.6(3)
N(1)-Mn(1)-N(5)	90.6(4)	N(2)-Mn(2)-N(7)'	86.3(4)
O(4)-Mn(1)-N(3)	94.8(4)	O(3)-Mn(2)-N(4)	99.4(3)
O(1)-Mn(1)-N(3)	158.6(3)	O(1)-Mn(2)-N(4)	157.0(3)
O(2)-Mn(1)-N(3)	87.7(3)	O(5)-Mn(2)-N(4)	83.9(4)
N(1)-Mn(1)-N(3)	76.0(4)	N(2)-Mn(2)-N(4)	75.3(3)
N(5)-Mn(1)-N(3)	92.4(4)	N(7)'-Mn(2)-N(4)	93.3(4)

atom N(7)' at x−1,y,z.

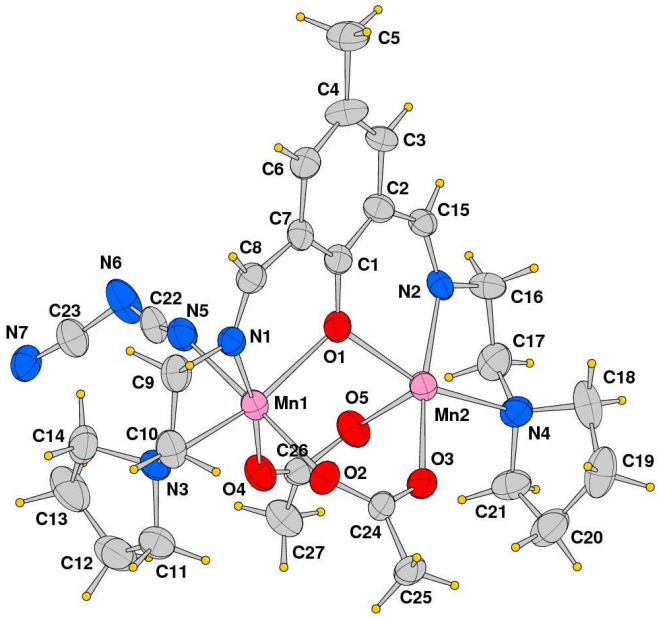

Fig. 5 ORTEP drawing (ellipsoid probability at 30%) with atom labels of the crystallographic independent unit of compound **3.**

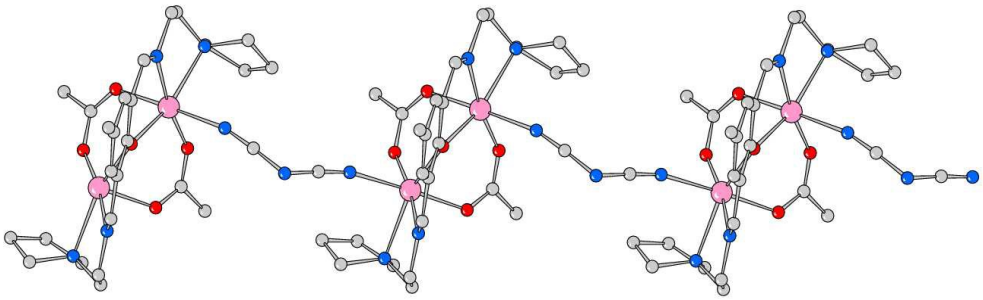

Fig. 6 Polymeric structure of compound **3** developed along axis *a*.

Catecholase-Like Activity:

Catechol oxidase, a type-3 copper protein can bind oxygen reversibly at room temperature and so it can be used to oxidize catechols to respective quinones. As a model of the enzyme here we have taken the three complexes of Mn(II). In order to mimic the functional property of the model compounds the most widely accepted substrate is 3, 5-di-*tert*-butylcatechol (3,5-DTBC) since its reduction potential for the quinone-catechol couple is low which makes it easy to be oxidized to

the corresponding quinone, 3, 5-di-*tert*-butyl-*o*-benzoquinone (3, 5-DTBQ) and at the same time due to presence of bulky substituents further oxidation and polymerization are stopped. Interestingly, all of the complexes exhibit extensive catalytic competence towards the oxidation of 3,5-DTBC to 3,5-DTBQ in the solvent DMSO. Moreover, the complex **2,** a binuclear Mn(II) Schiff base complex which shows a good catalytic efficiency towards the oxidation of catechols is the first reported di nuclear Mn(II) catalyst derived from compartmental Schiff base ligand . Before going on into detailed kinetic study we have checked the ability of the complexes to mimic the active site of catechol oxidase by treating 1×10^{-4} mol dm^{-3} solutions of the complexes with 1×10^{-2} mol dm^{-3} (100 equivalents) of 3,5-DTBC under aerobic condition. The time-dependent UV−vis spectral scan was executed in pure DMSO. Fig. 7, 8, 9 shows the spectral change for the complexes upon addition of 100-fold 3,5-DTBC (1×10^{-2} M) observed at interval of 5 minutes upto 30 minutes. The kinetics of the oxidation of 3,5-DTBC was determined by monitoring the increase of the concentration of the product 3,5-DTBQ and the experimental conditions were the same as were ported earlier.[5-8] All the complexes showed saturation kinetics and a treatment based on the Michaelis−Menten model seemed to be appropriate. The binding constant (K_M), maximum velocity (V_{max}), and rate constant for dissociation of substrates (i.e., turnover number, k_{cat}) were calculated for the complex by using the Lineweaver−Burk graph of 1/V vs1/[S] , using the equation $1/V = \{K_M/V_{max}\}\{1/[S]\} + 1/V_{max,}\}$, and the kinetic parameters are presented in Table 4 and in Table S1. From the data presented in Table 4 it may be inferred that the catalytic efficiency of our present Mn(II) complexes is comparable with highly active Mn based catalysts reported till date.

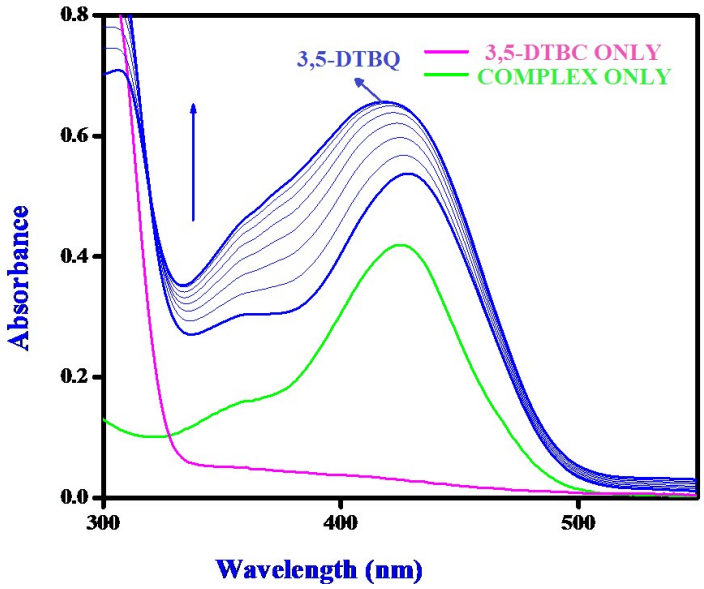

Fig. 7 Changes observed in UV−vis spectra of complex **1** in DMSO up to 30 minutes (conc. 1×10^{-4}M) upon addition of 100-fold 3,5-DTBC (1×10^{-2} M).

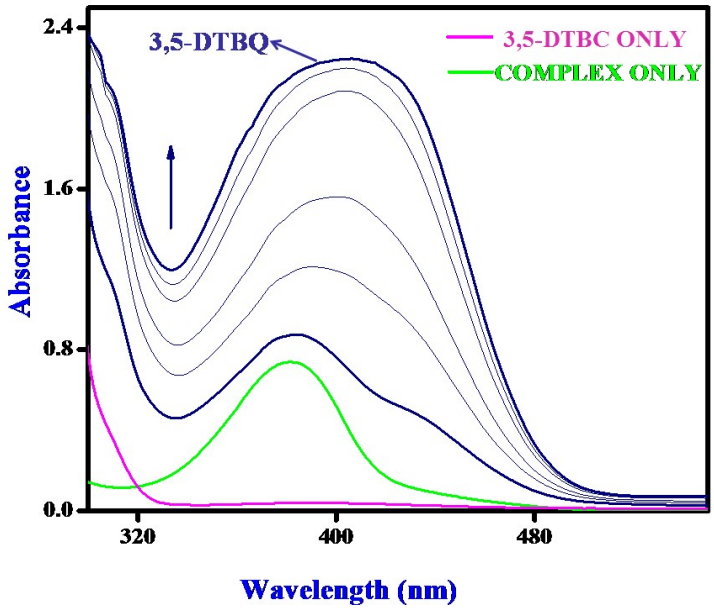

Fig. 8 Changes observed in UV−vis spectra of complex **2** in DMSO up to 30 minutes (conc. 1×10^{-4}M) upon addition of 100-fold 3,5-DTBC (1×10^{-2} M).

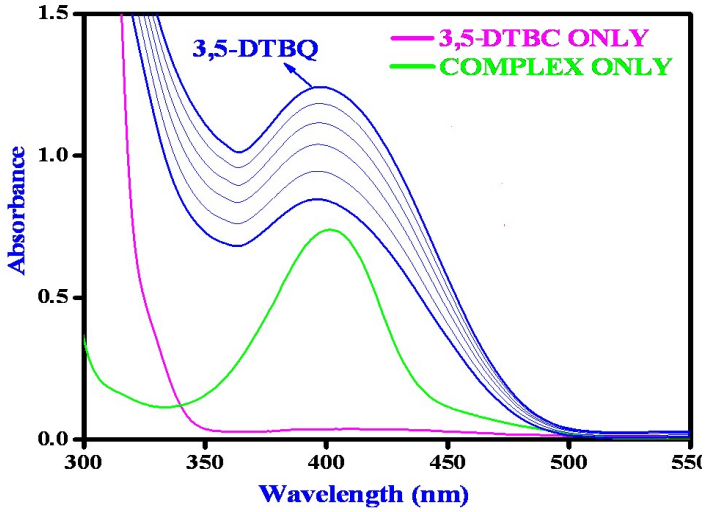

Fig. 9 Changes observed in UV−vis spectra of complex **3** in DMSO up to 30 minutes (conc. 1×10^{-4}M) upon addition of 100-fold 3,5-DTBC (1×10^{-2} M).

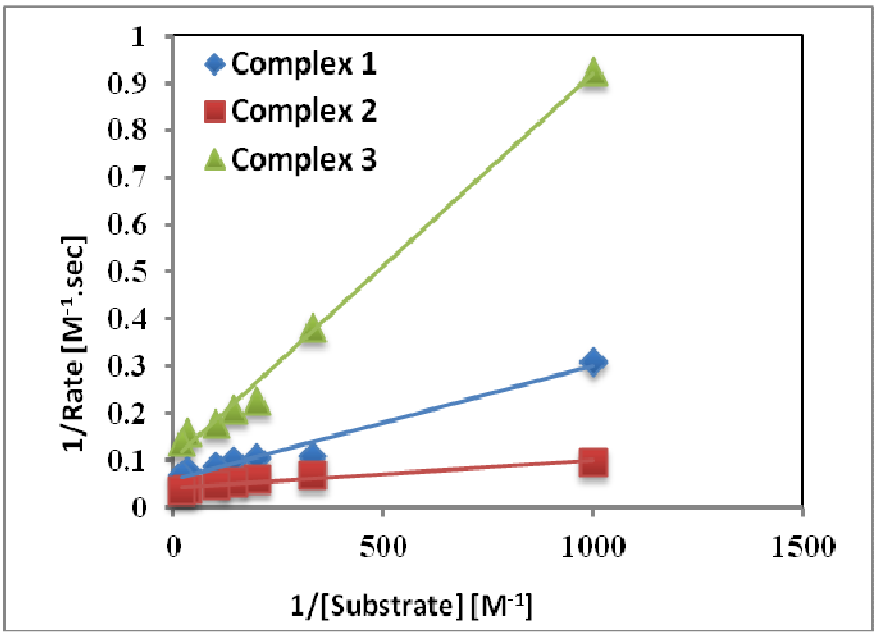

Fig. 10 Lineweaver−Burk plots for complexes **1, 2, 3** in DMSO medium for oxidation of Catechol.

Table 4. First Order Rate Constants for the Oxidation of Catechols by our complexes and the Similar Previously Reported Mn(II/III/IV), Ni(II), Cu(II) and Zn(II) Complexes using 3,5 DTBC as substrate.

Complex	Solvent	Metal present	Oxidation State	k_{cat} (in h^{-1})	Ref
$[Mn(L1)(SCN)_2(H_2O)]$	DMSO	Mn	(II)	607.08	This work
$[Mn_2(L1)(OAc)_2](BPh_4)]$,	DMSO	Mn	(II)	853.38	This work
$[Mn_2(L2)(OAc)_2(dca)]_n$	DMSO	Mn	(II)	255.19	This work
$[NiL^1(H_2O)_3]I_2 \cdot H_2O$ [a]	MeOH	Ni	(II)	9.27	9
$[NiL^1(H_2O)_3]Br_2 \cdot H_2O$ [a]	MeOH	Ni	(II)	8.48	9
$[Cu_2(H_2L2^2)(OH)(H_2O)(NO_3)](NO_3)_3 \cdot 2H_2O$ [b]	MeOH	Cu	(II)	32400	10
$[Cu(HL1^4)(H_2O)(NO_3)]_2(NO_3)_2 \cdot 2H_2O$ [b]	MeOH	Cu	(II)	14400	10
$[Cu(L1^1)(H_2O)(NO_3)]_2$ [b]	MeOH	Cu	(II)	10800	10
$[Cu_2(L2^3)(OH)(H_2O)_2](NO_3)_2$ [b]	MeOH	Cu	(II)	14400	10
$[Cu_2(L2^1)(N_3)_3]$ [b]	MeOH	Cu	(II)	28800	10
$[Cu_2(L1^1)(OH)(H_2O)(NO_3)_2]$ [c]	DMSO	Cu	(II)	73.70	11
$[Cu_2(L1^2)(OH)(H_2O)(NO_3)_2]$ [c]	DMSO	Cu	(II)	50.50	11
$[Cu(L2^1)(H_2O)(NO_3)]_2$ [c]	DMSO	Cu	(II)	84.60	11

$[Cu_2(L1^3)(OH)(H_2O)(NO_3)_2]$ [c]	DMSO	Cu	(II)	127.20	11
$[Cu_2(L1^4)(OH)(H_2O)(NO_3)_2]$ [c]	DMSO	Cu	(II)	49.60	11
$[Cu_2(L1^5)(OH)(H_2O)(NO_3)_2]$ [c]	DMSO	Cu	(II)	246.80	11
$[Cu_2(L1^6)(OH)(H_2O)(NO_3)_2]$ [c]	DMSO	Cu	(II)	50.70	11
$[Cu_2(L1^7)(OH)(H_2O)_2(NO_3)_2]$ [c]	DMSO	Cu	(II)	26.90	11
$[Cu_2(L1^9)(OH)(H_2O)(NO_3)_2]$ [c]	DMSO	Cu	(II)	51.80	11
$[Cu_2(L1^{10})(OH)(H_2O)(NO_3)_4]$ [c]	DMSO	Cu	(II)	68.30	11
$[Cu_2(L1^{12})(OH)(H_2O)(NO_3)_2]$ [c]	DMSO	Cu	(II)	50.10	11
$[Zn_2(H_2L^1)(OH)(H_2O)(NO_3)](NO_3)_3]$ [d]	MeOH	Zn	(II)	1060.00	12
$[Zn_2L^2Cl_3]$ [d]	MeOH	Zn	(II)	882.0	12
$[Zn_2L^3Cl_3]$ [d]	MeOH	Zn	(II)	297.00	12
$[Zn_2(L^4)_2(CH_3COO)_2]$ [d]	MeOH	Zn	(II)	352.00	12
$[MnL^1(OOCH)(OH_2)]$ [e]	MeCN	Mn	(III)	936.64	13a
$[MnL^2(OH_2)_2][Mn_2(L_2{}^2(NO_2)_3]$[e]	MeCN	Mn	(III)	365.34	13a
$[Mn_2L_2(NO_2)_2]$ [e]	MeCN	Mn	(III)	1432.74	13a
$[MnL^2Cl{\cdot}4H_2O]$ [f]	MeOH	Mn	(III)	247.00	13b
$[MnL^3Cl{\cdot}4H_2O]$[f]	MeOH	Mn	(III)	360.00	13b
$[MnL^4Cl{\cdot}4H_2O]$ [f]	MeOH	Mn	(III)	720.00	13b
$[Mn^{IV}{}_2(L^{1\bullet}{}_A)_2(L^{1\bullet\bullet})]$ [g]	CH_2Cl_2	Mn	(IV)	12.60	14a
$[Mn^{IV}(L^2{}_A)(L^{2\bullet})_2]$ [g]	CH_2Cl_2	Mn	(IV)	21.30	14a

$[Mn^{IV}(L^{3}_{A})(L^{3\bullet})_2]$ [g]	CH_2Cl_2	Mn	(IV)	55.20	14a
$[Mn^{IV}(L^{4}_{A})(L^{4\bullet})_2]$ [g]	CH_2Cl_2	Mn	(IV)	14.80	14a
$[Mn^{IV}(L^{5}_{A})(L^{5\bullet})_2]$ [g]	CH_2Cl_2	Mn	(IV)	34.14	14a
$[Mn^{IV}(L^{6}_{A})(L^{6\cdot})_2]$ [g]	CH_2Cl_2	Mn	(IV)	16.32	14a
$[Mn^{IV}(L^{7}_{A})(L^{7\cdot})_2]$ [g]	CH_2Cl_2	Mn	(IV)	15.60	14a
$[Mn(HL)(H_2O)_3](NO_3)_2\cdot(H_2O)]$ [h]	MeOH	Mn	(II)	2160.00	15
$[Mn(HL)(SCN)_2(H_2O)]\cdot 0.5H_2O]$ [h]	MeOH	Mn	(II)	1440.00	15
$[Mn(HL)(N(CN)_2)(H_2O)_2](NO_3)\cdot H_2O]$ [h]	MeOH	Mn	(II)	720.00	15

[a] L^1=2-[(2-Piperazin-1-ylethylimino)-methyl]phenol; [b] $L2^2$=2,6-bis(R-iminomethyl)-4-methyl-phenolato, R = *N*-ethylpiperazine [b]$L1^4$= 2-formyl-4-methyl-6R-iminomethyl-phenolato, R = *N*-ethylmorpholine, [b] $L1^1$=2-formyl-4-methyl-6R-iminomethyl-phenolato. R= *N*-propylmorpholine, [b] $L2^3$=2,6-bis(R-iminomethyl)-4-methyl-phenolato, R= *N*-ethylpyrrolidine, [b] $L2^1$=2,6-bis(R-iminomethyl)-4-methyl-phenolato; R=*N*-propylmorpholine,[c] $L1^1$=2,6-bis(R-iminomethyl)-4-chloro-phenolato, R= *N*-ethylpiperidine, [c] $L1^2$=2,6-bis(R-iminomethyl)-4-*t*-butyl-phenolato, R= *N*-ethylpiperidine, [c] $L2^1$=2-formyl-4-methyl-6R-iminomethyl-phenolato, R= *N*-ethylpiperidine, [c] $L1^3$=2,6-bis(R-iminomethyl)-4-chloro–phenolato, R = *N*-ethylmorpholine, [c]$L1^4$=2,6-bis(R-iminomethyl)-4-*t*-butyl–phenolato, R= *N*-ethylmorpholine, [c] $L1^5$=2,6-bis(R-iminomethyl)-4-chloro–phenolato, R=*N*-propylmorpholine, [c] $L1^6$=2,6-bis(R-iminomethyl)-4-*t*-butyl–phenolato, R=*N*-propylmorpholine, [c] $L1^7$=2,6-bis(R-iminomethyl)-4-chloro–phenolato, R= *N*-ethylpyrrolidine, [c] $L1^9$=2,6-bis(R-iminomethyl)-4-*t*-butyl–phenolato, R= *N*-ethylpyrrolidine, [c] $L1^{10}$=2,6-bis(R-iminomethyl)-4-chloro–phenolato, R = *N*-ethylpiperazine, [c] $L1^{12}$=2,6-bis(R-iminomethyl)-4-*t*-butyl–phenolato, R = *N*-ethylpiperazine, [d] L1=2,6-bis(R-iminomethyl)-4-methyl-phenolato, R = *N*-ethylpiperazine [d] L2=2,6-bis(R-iminomethyl)-4-methyl-phenolato, R = *N*-ethylpyridine, [d] L3=2,6-bis(R-iminomethyl)-4-methyl-phenolato, R= *N*-ethylpyrrolidine, [d] L4=2,6-bis(R-iminomethyl)-4-methyl-phenolato, R= benzylamine, [e] L^1= 2,7-bis(2-hydroxyphenyl)-2,6-diazaocta-2,6-diene, [e] L^2= 1,7-bis(2-hydroxyphenyl)-2,6-diazahepta-1,6-diene); [f] L^2= *N,N*'-1-methylethylenebis(3-formyl-5-methylsalicylaldimine), [f] L^3= *N,N*'-1,1-dimethylethylenebis(3-formyl-5-methylsalicylaldimine), [f] L^4= *N,N*¢-cyclohexenebis(3-formyl-5-methylsalicylaldimine); [g] L^1=1,3-Bis(4,6-di-*tert*-butyl-2-iminophenol)benzene, [g] L^2= 2-anilino-4,6-di-*tert*-butylphenol, [g] L^3= 2-(3,5-di *t*-butyl-anilino)-4,6-di-*tert*-butylphenol, [g] L^4= 2-(3,5-di-trifluromethane-anilino)-4,6-di-*tert*-butylphenol, [g] L^5 =2-(3,5-di methyl-anilino)-4,6-di-*tert*-butylphenol, [g] L^6 =2-(3,5-di chloro-anilino)-4,6-di-*tert*-butylphenol, [g] L^7 =2-(3,5-di methoxy-anilino)-4,6-di-*tert*-butylphenol; [h] HL = 2,6-bis{2-(N-ethyl)pyridineiminomethyl}-4-methylphenolato,

Mechanistic interpretation on catecholase activity exhibited by the complexes.

Earlier our group tried to explore the origin of Catecholase like activity exhibited by Mn(II) and Mn(III) with Schiff Base ligands.[13b,15] In case of Mn(III) we are able to prove that the origin of the activity was related to metal center Redox participation, where Mn(III) underwent reduction to Mn(II) with concomitant oxidation of catechol to quinone. However with the case of Mn(II)

complex we failed to evaluate the plausible mechanism for the catecholase activity. The oxidation from catechol to quinone may occured via three pathways (i) metal centered reduction, (ii) ligand centered imine radical formation (iii) phenoxy radical formation in case of phenolic ligands. So in this present work we tried to evaluate the correct pathway with the help of EPR and electrochemical studies. As the three complexes are of same kind we selected the dinuclear one (**2**) as a model for EPR spectroscopic analysis. For this, we have prepared a 1:100 mixture of complex **2** and 3,5-DTBC (10^{-1} M) in DMSO solvent and recorded the EPR spectra within 2 min of mixing. A characteristic six line EPR spectrum (Fig. 11) corroborates the Mn (II) species when the complex **2** is dissolved in DMSO. An additional sharp peak (g=1.99) (Fig. 12) appears after mixing the complex with 3,5-DTBC which indicates the formation of ligand-centered imine radical and that radical formation is most probably responsible for the catalytic oxidation of 3,5-DTBC to 3,5-DTBQ in presence of aerial oxygen. We have also performed the EPR experiment at 77 K at power saturation condition to find out any signal at the half-filed but our repeated attempts failed to distinguish any characteristic signal. However, our present EPR study implies that when the Mn(II) complex is mixed with 3,5-DTBC, the ligand part most probably the imine bond of the coordinated ligand undergoes reduction with concomitant oxidation of the catechol to quinone via the formation of semibenzoquinone radical, a similar observation as we found in our earlier study with our Zn complex.[12]

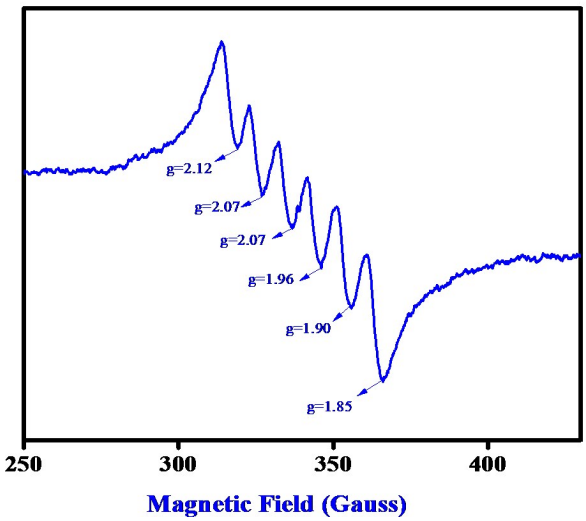

Fig. 11 EPR spectrum of complex **2** in DMSO medium at 77 K.

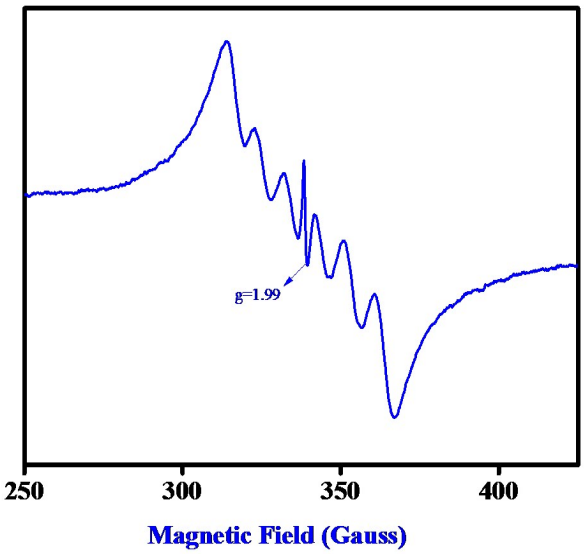

Fig. 12 EPR spectrum of a 1:100 mixture of complex **2** and 3,5-DTBC (10^{-1} M) in DMSO at 77 K.

Interestingly, when this catalytic oxidation was performed in an inert atmosphere, no 3,5-DTBQ formation was noticed. However, upon exposure of the reaction mixture in dioxygen atmosphere immediately 3,5-DTBQ formation was observed. This observation indeed indicates that dioxygen is one of the active participants in the catalytic cycle; it converts the semibenzoquinone radical, formed in the first step of catalysis, to the quinone with subsequent regeneration of the catalyst.

Electrochemical Study

All the Mn(II) complexes show an irreversible reduction at −0.72 vs Ag/AgCl, which we tentatively assign to imine reduction of the ligand moiety. On the oxidative side the mononuclear Mn(II) complex exhibits one irreversible oxidation at 0.89 V, which is probably due to oxidation of phenolate to phenoxyl radical. The binuclear complexes show two distinctive oxidation peaks, both the processes being irreversible in nature. For complex **2**, the anodic peak potentials are at 0.96 and 1.12 V (Fig. S13), whereas for **3**, the corresponding values are 0.51 and 1.07 V (Fig. S15). We tentatively assign the first anodic peak to Mn(II)/Mn(III) oxidation and second peak to oxidation of phenolate moiety of the ligand. Now we performed the cyclic voltammetic study of the complexes in presence of 3,5-DTBC. All three complexes exhibit nearly similar response and

the thus the behavior of complex 1 in presence of 3,5-DTBC is stated here. On addition of 3,5-DTBC to a solution of complex **1** the current height of the imine reduction peak at −0.68V decreases, while a new peak appears at −0.29V may be due to reduction of coordinated semiquinone to catechol. (Fig. 13) On the oxidative side a very strong peak at ~0.8 V corresponds to formation of semiquinone is observed without any signal responsible for the oxidation of Mn(II) to Mn(III) (Fig. S15 and S16). Thus the cyclic voltammetry data confirms that reduction of the complex during 3,5-DTBC oxidation can take place only at the imine part of the ligand and the metal center is no way involved in this process.

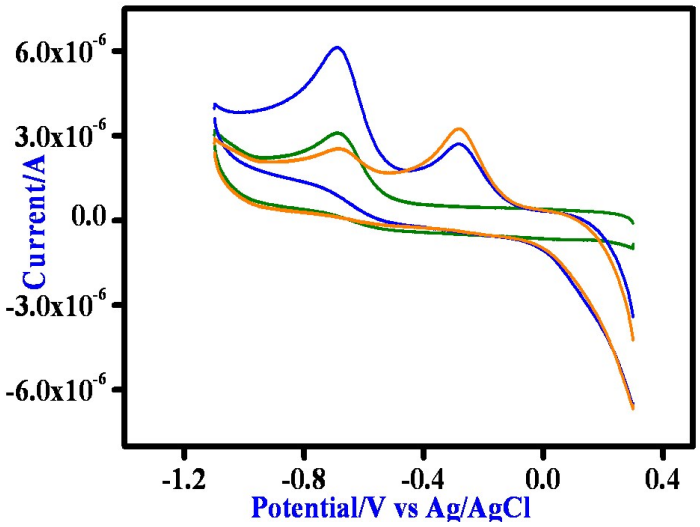

Fig. 13 Time dependent CV spectrum of complex **1** after addition of DTBC at the GC electrode in DMSO medium at 100 mV s^{-1} scan rate as representative.

On the basis of the results obtained from EPR and cyclic voltametric studies a plausible mechanism has been proposed in Scheme 2. With the dinuclear complexes two catechol molecules are oxidized per cycle, whereas only one is oxidized by the monomeric Mn(II) complex. Here the mononuclear complex **1** is presented for simplicity.

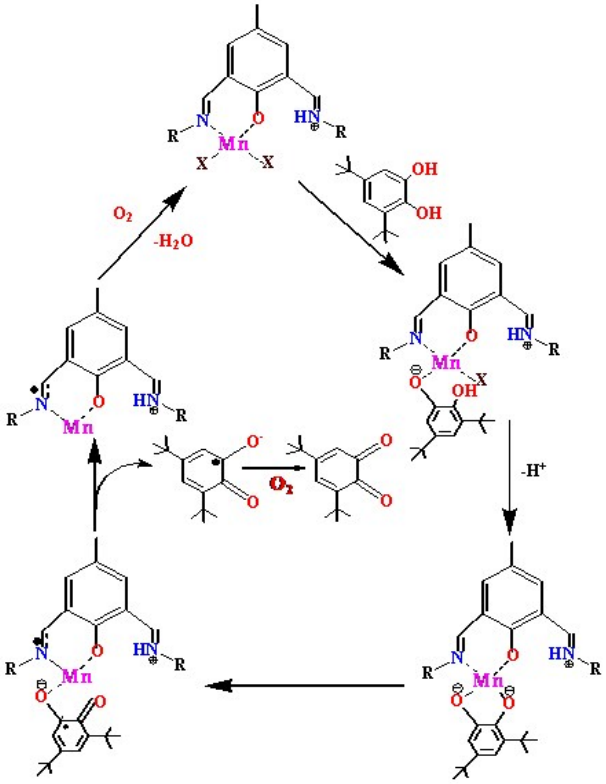

Scheme 2. Proposed mechanism for the catalytic cycle of oxidation of 3,5-DTBC by mononuclear Mn(II) complex.

Magnetic Properties of Complex 2 and 3.

The magnetic properties of complex **2** and **3**, in the form of $\chi_M T$ (χ_M is the susceptibility per dinuclear unit) *vs.* T plots, are shown in Fig. 14 in a temperature range 5-300 K for **2** and 2-300 K for **3**, respectively. The observed $\chi_m T$ values at room temperature, 8.76 emu K mol^{-1} (μ_{eff} = 8.37 μ_B) and 8.39 emu K mol^{-1} (μ_{eff} = 8.19 μ_B) for **2** and **3**, respectively are comparable with the spin-only value of 8.75 emu K mol^{-1} (μ_{eff} =8.37 μ_B), expected for two independent high-spin Mn(II) ions [(S_{Mn}, S_{Mn}) = (5/2, 5/2) assuming g = 2.0]. As the temperature is lowered, the $\chi_m T$ values decrease in a monotonous manner and become 0.39 emu K mol^{-1} for **2** at 5 K and 0.31

emu K mol^{-1} for **3** at 2 K. This result indicates the presence of an antiferromagnetic spin-exchange interaction between Mn (II) ions.

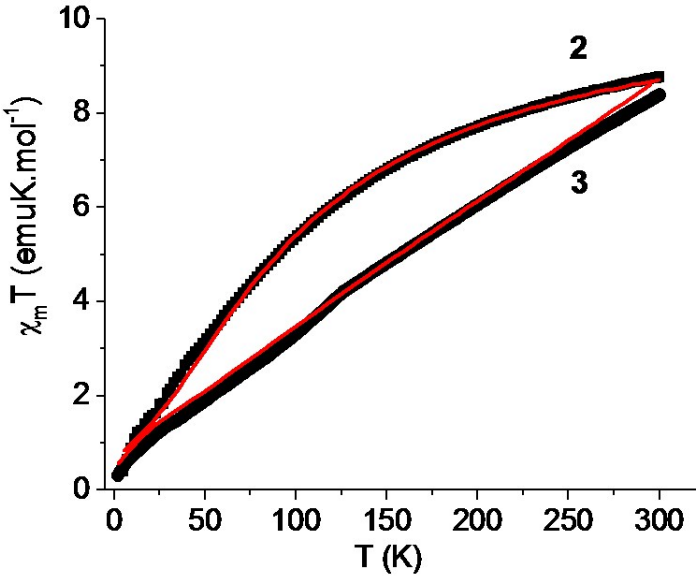

Fig. 14 Temperature variation of the magnetic susceptibilities of **2** and **3** as χT versus T plots (The solid line represents the best fit of the experimental data based on the Heisenberg model).

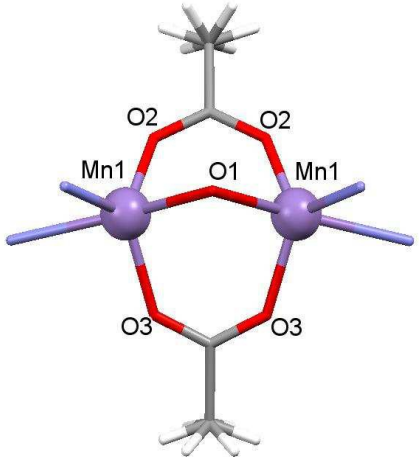

Fig. 15 Local coordination environments of Mn(II) atoms and the magnetic exchange coupling pathway for complex **2**.

For dinuclear Mn(II) complexes (S_1=S_2=5/2), the theoretical expression of the magnetic susceptibility based on the Heisenberg Hamiltonian($\boldsymbol{H}=-2J\boldsymbol{S}_1\boldsymbol{S}_2$)is:

$$\chi T=\frac{2N g^2 \mu_B^2}{k}\times\frac{\left[55+30e^{-10J/kT}+14e^{-18J/kT}+5e^{-24J/kT}+e^{-28J/kT}\right]}{\left[11+9e^{-10J/kT}+7e^{-18J/kT}+5e^{-24J/kT}+3e^{-28J/kT}+e^{-30J/kT}\right]}\times(1-\rho)+\frac{N g^2 \mu_B^2}{k}S(S+1)\rho+N_\alpha T \quad \text{(Eq.1)}$$

In these expression, ρ presents the fraction of paramagnetic impurity in the sample, Nα is a temperature independent paramagnetism and the other symbols have their usual meanings. To determine the exchange parameters, χT was fitted using Eq.1 for the range 5–300 K gives the best agreement with the experimental data for J = - 9.15 cm^{-1}, g = 2.01, ρ= 0.09 and Nα= 0.00089 (R^2=0.99802) for complex **2**.

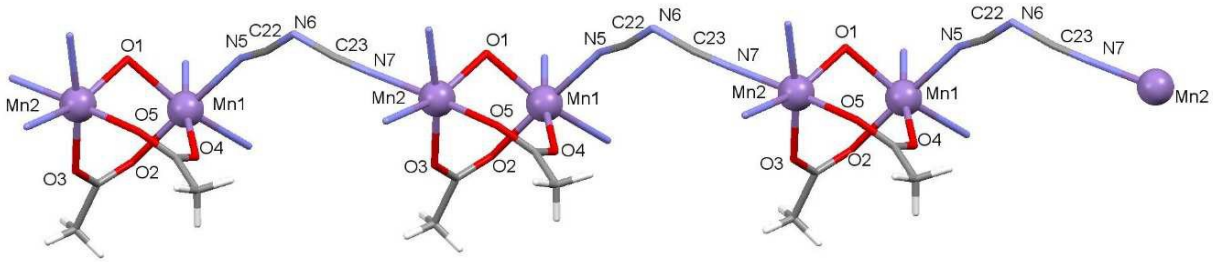

Fig. 16 Local coordination environments of Mn(II) atoms and the magnetic exchange coupling pathway for complex **3**.

The complex **3** is a one-dimensional chain and its magnetic interactions should be expressed using alternating exchange interactions, namely, Mn–J–Mn–J′–Mn–J–Mn–J′–Mn, in which J represents the intradimer exchange interaction via the triple oxygen bridges whereas J′ is the interdimer exchange interaction via dicyanamide bridge in the chain (Fig. 16). To take into account the interaction between the dimer entities, the susceptibility can be corrected by the molecular field approximation[20] (Eq. (2) where zJ' denotes the intra-molecular exchange parameter.

$$\chi_M T = \frac{\chi T}{1 - \chi\left(2zJ'/Ng^2\beta^2\right)} \qquad \text{(Eq.2)}$$

In these expression, z is the number of nearest-neighbouring dimers (in this case z = 2) and J' accounts for the presence of magnetic interactions between neighboring dimers and the other symbols have their usual meanings. To determine the exchange parameters, χT was fitted using Eq.2 for the range 2-300 K gives the best agreement with the experimental data for J = -46.89cm^{-1}, J'= - 2.38, g = 2.20, ρ= 0.025and Nα= 0.00046 (R^2=0.99852) for complex **3**.

The overall magnetic behavior of the complex **2** and **3** is dominated by antiferromagnetic interaction between the spin carriers and resembles that of related compounds.[16-19]

Experimental Section

Physical methods and materials. 3,5 di-*tert*-butyl catechol was purchased from Sigma-Aldrich. Reaction solutions for 3,5-DTBC was prepared according to the standard sterile techniques.
Elemental analyses (carbon, hydrogen, and nitrogen) were performed using a PerkinElmer 240C analyzer. Infrared spectra (4000−400 cm^{-1}) were recorded at 28 °C on a Shimadzu FTIR-8400S and PerkinElmer Spectrum Express Version 1.03 using KBr pelletsas mediums. UV−visible spectra and kinetic traces were monitored with a Shimadzu UV-2450PC spectrophotometer equipped with multiple cell-holders and thermostat. Magnetic susceptibility measurements over the temperature range 2−300 K was performed at a magnetic field of 0.0750 T using a Quantum Design SQUID MPMSXL-5 magnetometer. Correction for the sample holder, as well as the diamagnetic correction, which was estimated from the Pascal constants.[20],[21] EPR experiments were performed at liquid nitrogen temperature (77 K) in methanol, using a JEOL JES-FA200 spectrometer at X band (9.13 GHz).
Cyclic voltammetric and DPV measurements were performed by using a CH1106A potentiostat with glassy carbon (GC) as working electrode, Pt-wire as counter electrode and Ag, AgCl/sat KCl as reference electrode. All solutions were purged with dinitrogen prior to measurements.

High-purity N-(2-aminoethyl)-pyrrolidine, N-(2-aminoethyl)morpholine, were purchased from commercial sources (Fluka, Lancaster Chemical Co. Inc., Aldrich) and used as received. The 2,6-diformyl-4-R-phenols (R = methyl,chloro) were prepared according to the literature method.[22] MeOH was dried over CaH_2 for 2 days and then distilled under reduced pressure prior to use. Water used in all physical measurement and experiments was Milli-Q grade. All other chemicals used were of AR grade.

Synthesis of the Complexes.

The following general template synthetic route was adopted for preparing all complexes. A methanolic solution of the manganese salt was added to the ligand solution formed *in situ* via condensation of 2,6-diformyl-4-R-phenol (where R= methyl, chloro) with the corresponding amines maintaining the same molar ratio. The preparation, composition, and other physicochemical characteristics of all complexes using the template technique are given below.

Syntheses.

$[Mn(L1)(SCN)_2(H_2O)]$, (**1**)

To a methanolic solution (5 mL) of N-(2-aminoethyl)morpholine (0.260 g, 2 mmol) a methanolic solution (10 mL) of 4-chloro-2,6-diformylphenol (0.180 g,1 mmol) was added dropwise, and the mixture was refluxed for 30 minutes. Then a methanolic solution (15 mL) of manganese chloride (0.604 g, 2.5 mmol) was added to it, and the resulting mixture was allowed to reflux for additional 2 h. The deep brown solution was filtered and cooled to room temperature. Then an aqueous solution of sodium thiocyanate (0.32g, 4 mmol) was added to the reaction mixture and stirred for about 30 minutes. The resulting solution was filtered and the filtrate was kept in a $CaCl_2$ dessicator. Deep brown crystals suitable for X-ray data collection were obtained from the filtrate on keeping the solution overnight (yield 75%). Anal. Calcd for $C_{22}H_{31}Mn_1N_6O_4S_2Cl$: C (44.14%); H (5.5%); N (14.04%); Found: C (44.94%); H (5.89%); N (14.1%); FT-IR data (KBr pellet): I.R: ν(C=N) 1641 cm^{-1}; ν(skeletal vibration) 1533 cm^{-1}; ν(SCN^-) 2065 cm^{-1}; UV/vis (MeOH): $\lambda_{max}(\varepsilon)$ = 425nm(4200 L mol^{-1} cm^{-1}).

$[Mn_2(L1)(OAc)_2](BPh_4)]$, **(2)**

To a methanolic solution (5 mL) of N-(2-aminoethyl)morpholine (0.260 g, 2 mmol) a methanolic solution (10 mL) of 4-chloro-2,6-diformylphenol (0.180 g,1 mmol) was added in a dropwise manner, and the mixture was refluxed 30 min. Then a methanolic solution (15 mL) of manganese acetate (0.604 g, 2.5 mmol) was added to it, and the resulting mixture was allowed to reflux for 2 h. The deep brown solution was filtered and cooled to room temperature. Then an aqueous solution of tetra phenyl borate (0.88 g, 4 mmol) was added to the reaction mixture and stirred for about 10 min. The resulting solution was filtered and the filtrate was kept in a $CaCl_2$ dessicator. Deep brown crystals suitable for X-ray data collection were obtained from the filtrate after few days. (yield 70%).

Anal. Calcd for $C_{48}H_{34}Mn_2N_4O_7BCl$: C (60.30%); H (3.55%); N (5.75%); Found: C (60.50%); H (3.95%); N (5.29%); FT-IR data (KBr pellet): I.R: ν(C=N) 1643 cm^{-1}; ν(skeletal vibration) 1537 cm^{-1}; ν(OAc^-) 1483 cm^{-1}; UV/vis (MeOH): λmax(ε) = 381nm(7390 L mol^{-1} cm^{-1}).

$[Mn_2(L2)(OAc)_2(dca)]_n$**, (3)**

To a methanolic solution (5 mL) of N-(2-aminoethyl)pyrrolidine (0.228 g, 2 mmol) a methanolic solution (10 mL) of 4-methyl-2,6-diformylphenol (0.164 g,1 mmol) was added in a dropwise manner, and the mixture was refluxed for 30 min. Then a methanolic solution (15 mL) of manganese acetate (0.604 g, 2.5 mmol) was added to it, and the resulting mixture was allowed to reflux for 2 h. The deep brown solution was filtered and cooled to room temperature. Then to the reaction mixture an aqueous solution of sodium dicyanamide (0.284 g, 4 mmol) was added continuing to stir for about 30 min. The resulting solution was filtered and the filtrate was kept in a $CaCl_2$ dessicator. Deep brown crystals suitable for X-ray data collection were obtained from the filtrate after keeping the solution overnight (yield 68%).

Anal. Calcd for $C_{27}H_{37}Mn_2N_7O_5$: C (49.88%); H (5.69%); N (15.08%); Found: C (49.50%); H (5.95%); N (15.37%); FT-IR data (KBr pellet): I.R: ν(C=N) 1641 cm^{-1}; ν(skeletal vibration) 1533 cm^{-1}; ν(OAc^-) 1488 cm^{-1} ν($N(CN)_2^-$) 2165 cm^{-1} ; UV/vis (MeOH): λmax(ε) = 407nm(7530 L mol^{-1} cm^{-1}).

X-ray Data Collection and Structure Determination. Data collection of the structures reported was carried out at room temperature on a on a Bruker Smart CCDdiffractometer (**1**-**2**) and on a Nonius DIP-1030H system (**3**), all equipped with graphite-monochromated Mo-Kα radiation (λ=0.71073 Å). Cell refinement, indexing and scaling of the data set were carried out using Bruker Smart Apex and Bruker Saint packages,[23] Mosflm and Scala.[24]All the structures were solved by direct methods and subsequent Fourier analyses[25]and refined by the full-matrix least-squares method based on F^2 with all observed reflections.[25]In compound **1**the coordinated morpholine moiety was found disordered over two positions (occupancies refined at 0.537(6)/0.463(6) with a restrainedgeometry).All the calculations were performed using the WinGX System, Ver 1.80.05.[26] Pertinent crystallographic data and refinement details are summarized in Table 5.

Table 5. Crystallographic Data and Details of Refinements for Complexes **1**-**3**.

	1	**2**	**3**
Empirical formula	$C_{22}H_{31}ClMnN_6O_4S_2$	$C_{48}H_{54}BClMn_2N_4O_7$	$C_{27}H_{37}Mn_2N_7O_5$
MW	598.04	955.09	649.52
Crystal system	Monoclinic	Monoclinic	Triclinic
Space group	$P\,2_1/c$	$P\,2_1/m$	$P\bar{1}$
a /Å	9.1058(4)	11.1317(17)	10.058(3)
b /Å	21.8162(9)	24.757(4)	12.348(3)
c /Å	14.3490(6)	17.083(3)	13.366(4)
α /°			78.53(2)
β /°	97.9080(10)	93.100(2)	84.51(3)
γ /°			70.55(2)
V /Å^3	2823.4(2)	4700.9(12)	1533.3(7)
Z	4	4	2
Dcalc /g cm^{-3}	1.407	1.349	1.407
μ /mm^{-1}	0.748	0.648	0.870
F(000)	1244	1992	676
Theta range /°	1.71 - 25.57	1.19 - 26.39	1.56 - 23.26
Total data	32565	32933	11533
Unique data	5273	9482	4339

*R*int	0.0325	0.0398	0.0779
Reflections$I>2\sigma(I)$	4223	6350	1478
Parameters	395	592	370
Goodness-of-fit	1.022	1.038	0.825
R_1[a]	0.0331	0.0557	0.0731
wR_2 ($I>2\sigma(I)$) [a]	0.0849	0.1675	0.1723
Residuals /e Å^{-3}	0.285, –0.247	0.981, –0.399	0.364, –0.362

[a] $R1 = \Sigma\, ||Fo|-|Fc|| \,/\, \Sigma|Fo|$, $wR2 = [\Sigma w\,(Fo^2 - Fc^2)^2 / \Sigma w\,(Fo^2)^2]^{½}$

[b] CCDC-1425706 -1425708 contain the supplementary crystallographic data for this paper.

Conclusion

Three manganese(II) complexes having different nuclearities, one mono-, one di- and one dinuclear based polynuclear, have been synthesized using two "end-off" compartmental Schiff-base ligands, HL1 and HL2. Protonation of one of the imine nitrogen of HL1 in presence of SCN as co-ligand cancel out the possibility of metalation in the second compartment of HL1 leads to mononuclearity. In presence of acetate as co-ligand and BPh_4 as counter anion HL1 generates dinuclear complex **2**. HL2 in presence of acetate and dca as co-ligands forms acetate bridged dinuclear based polynuclear complex where dca bridges two dinuclear units. All three complexes have been structurally characterized and oxidation state of each of the manganese is +2 as is evidenced from magnetic susceptibility and EPR study. Variable temperature magnetic study implies the presence of an antiferromagnetic spin-exchange interaction between Mn(II) ions with J = - 9.15 cm^{-1} and J = - 46.89 cm^{-1} for complex **2** and **3**, respectively. All three complexes exhibit catecholase-like activity towards 3,5-DTBC as model substrate with varying degree, **2**>**1**>**3**. In order to unveil the origin of catecholase activity whether related to metal centered redox participation or radical generation we have performed EPR and cyclic voltametric studies. EPR investigation of the solution of 3,5-DTBC and complex suggests radical formation. Cyclic voltametric study suggests ligand centered reduction rather than the reduction of Mn(II) to Mn(I). It is therefore concluded that catecholase-like activity of the present Mn(II) complexes is following radical pathway as is observed in analogous Zn(II) and Ni(II) complexes.

Acknowledgements

The authors wish to thank CSIR, New Delhi [01(2464)/11/EMR-II dt16-05-11 to D.D.], for financial support and the University of Calcutta for providing the facility of the single-crystal X-ray diffractometer from the DST FIST program and for collecting variable temperature magnetic study from SQUID-VSM in CRNN. Authors are also thankful to Prof. Shyamal Kumar Chattopadhyay of IIEST, Shibpur for providing the facilities of electrochemical studies. I.M is thankful to UGC [UGC/729/Jr Fellow(Sc)] for providing fellowship.

References

1 M. Fontecave, J-L. Pierre, *Coord Chem Reviews*., 1998, **170**, 125.

2 L. Que Jr, W. B. Tolman, *NATURE*., 2008, **455**, 333.

3 J. Suh, *Acc. Chem. Res.,* 1992, **25**, 273.

4 P. Chaudhuri, M. Hess, U. Flörke, K. Wieghardt, *Angew. Chem.* 1998, **37**, 2217.

5 J. Reim, B. Krebs, *J. Chem. Soc*., *Dalton Trans*., 1997, 3793.

6 S. Torelli, C. Belle, I. Gautier-Luneau, J. L. Pierre, E. Saint-Aman, J. M. Latour, L. Le Pape, D. Luneau, *Inorg. Chem*., 2000, **39***,* 3526.

7 A. Neves, L. M. Rossi, A. J. Bortoluzzi, B. Szpoganicz, C. Wiezbicki, E. Schwingel, *Inorg. Chem*., 2002, **41**, 1788.

8 J. Mukherjee, R. Mukherjee, *Inorg. Chim. Acta*., 2002, **337**, 429.

9 J. Adhikary, P. Chakraborty, S. Das, T. Chattopadhyay, A. Bauzá, S. K. Chattopadhyay, B. Ghosh, F. A. Mautner, A. Frontera, D. Das, *Inorg. Chem*., 2013, **52**, 13442.

10 K. S. Banu, T. Chattopadhyay, A. Banerjee, S. Bhattacharya, E. Suresh, M. Nethaji, E. Zangrando, D. Das, *Inorg. Chem*., 2008, **47**, 7083.

11 P. Chakraborty, J. Adhikary, B. Ghosh, R. Sanyal, S. K. Chattopadhyay, A. Bauzá, A. Frontera, E. Zangrando, D. Das, *Inorg. Chem.*, 2014, **53**, 8257.

12 A. Guha, T. Chattopadhyay, N. D. Paul, M. Mukherjee, S. Goswami, T. K. Mondal, E. Zangrando, D. Das, *Inorg. Chem.*, 2012, **51**, 8750.

13 (a) P. Seth, M.G.B. Drew, A. Ghosh, *Journal of Mol. Cata. A: Chemical*., 2012, **365**,154. (b) K. S. Banu, T. Chattopadhyay, A. Banerjee, M. Mukherjee, S. Bhattacharya, G. K. Patra, E. Zangrando, D. Das, *Dalton Trans.*, 2009, 8755.

14 (a) S. Mukherjee, T. Weyherm¨uller, E. Bothe, K. Wieghardt, P. Chaudhuri, *Dalton Trans ,* 2004, 3842. (b) S. Mukherjee, E. Rentschler, T. Weyhermüller, K. Wieghardt, P. Chaudhuri, *Chem. Commun.*, 2003, 1828.

15 A. Guha, K. S. Banu, A. Banerjee, T. Ghosh, S. Bhattacharya, E. Zangrando, D. Das, *Journal of Mol. Cata. A: Chemical*., 2011, **338**, 51.

16 C. S. Hong **,** Y. Do, *Inorg. Chem.,* 1997**, 36***,* 5684.

17 A. Escuer, R. Vicente, M. A. S. Goher, F. A. Mautner, *Inorg. Chem.* 1996**, 35***,* 6386.

18 J. L. Manson, C. D. Incarvito, A. L. Rheingold, J. S. Miller, *J. Chem. Soc*., *Dalton Trans*., 1998, 3705.

19 M A. Kiskin, I. G. Fomina, G. G. Aleksandrov, A. A. Sidorov, V. M. Novotortsev, Y.V. Rakitin, Z. V. Dobrokhotova, V. N. Ikorskii, Y. G. Shvedenkov, I. L. Eremenko, I. I.Moiseev, *Inorg. Chem. Comm*., 2005, ***8***, 89.

20 C.J. O'Connor, *J.Prog. Inorg. Chem*, 1982, **29**, 203.

21 G. A. Bain, J. F. Berry, *J. Chem. Educ.,* 2008, **85**, 532.

22 R. R. Gagne, C. L. Spiro, T. J. Smith, C. A. Hamann, W. R. Thies, A. K. Shiemeke, *J. Am. Chem. Soc.,* 1981, **103**, 4073.

23 SMART, SAINT. Software Reference Manual; Bruker AXS Inc.: Madison, WI, 2000.

24 Collaborative Computational Project, Number 4. Acta Crystallogr., Sect. D 50 1994, 760.

25 G. M. Sheldrick, *Acta Crystallogr*., Sect. A. 2008, **64**, 112.

26 L. J. Farrugia, *J. Appl. Crystallogr*., 2012, **45**, 849.

Graphical Abstract

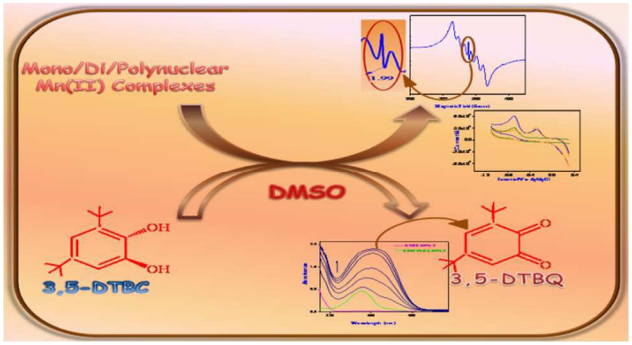

The origin of catecholase-like activity of Mn(II)-Schiff-base complexes has been explored on studying structurally characterized mono-, di- and polynuclear Mn(II) complexes of two “end-off” compartmental Schiff-base ligands. EPR and CV experiments are in favor of ligand centered radical formation rather than metal centered redox participation for that activity.